



A simple-to-use nomogram for predicting the risk of radiation pneumonitis in patients with thoracic segment esophageal squamous cell carcinoma

Ting Qiu[#], Yuxia Deng[#], Haochun Guo, Haijun Zhang

Department of Oncology, Zhongda Hospital, Medical School of Southeast University, Nanjing, China

Contributions: (I) Conception and design: T Qiu, H Zhang; (II) Administrative support: H Zhang, Y Deng; (III) Provision of study materials or patients: H Guo, T Qiu, Y Deng; (IV) Collection and assembly of data: T Qiu, Y Deng; (V) Data analysis and interpretation: T Qiu; (VI) Manuscript writing: All authors; (VII) Final approval of manuscript: All authors.

[#]These authors contributed equally to this work.

Correspondence to: Haijun Zhang. Department of Oncology, Zhongda Hospital, Medical School of Southeast University, 87 Dingjiaqiao Road, Nanjing 210009, China. Email: haijunzhang@seu.edu.cn.

Background: Radiation pneumonitis (RP) is one of the most severe complications of radiotherapy (RT) or concurrent chemoradiotherapy for thoracic segment esophageal squamous cell carcinoma (TSESCC) with delayed diagnose by conventional computed tomography (CT). The study aimed to develop a nomogram to predict the risk of RP early.

Methods: Data was collected from 174 patients with clinicopathologically confirmed TSESCC from October 2013 to June 2020. Procalcitonin (PCT), C-reactive protein (CRP), and interleukin-6 (IL-6) levels in serum were dynamically monitored during radiotherapy. Lasso analysis was used for feature screening before multivariate logistic regression analysis to reduce the multicollinearity of variables. A nomogram combined with biological factors and clinical signs for individualized risk assessment and precise prediction of RP was developed and assed the performance with respect to its calibration, discrimination.

Results: Of the 174 patients, 30 patients developed RP (grade ≥ 2) while 144 patients did not. After variable screening by Lasso analysis and logistics multivariate regression analysis, the predictor variables that were finally retained in the nomogram prediction model included IL-6, CRP, and radiotherapy techniques. The model displayed good discrimination with an area under the curve (AUC) of 0.898 (95% CI: 0.849–0.947), with the sensitivity and specificity of 0.967 and of 0.736, respectively. This model also shows good calibration and clinical practical value. In addition, the study provided a web-based version of the dynamic nomogram to facilitate clinical application.

Conclusions: The study provides a nomogram model containing IL-6, CRP, RT techniques, which could be conveniently used for individualized prediction of RP in patients with TSESCC during radiotherapy or concurrent chemoradiotherapy.

Keywords: Radiation pneumonitis (RP); esophageal cancer (EC); interleukin-6 (IL-6); C-reactive protein (CRP); nomogram

Submitted Mar 06, 2022. Accepted for publication Jul 22, 2022.

doi: 10.21037/tcr-22-582

View this article at: <https://dx.doi.org/10.21037/tcr-22-582>

Introduction

Esophageal cancer (EC) was ranked as the eighth most frequently diagnosed cancer and the sixth leading cause of cancer-related deaths in 2020 worldwide (1). Definitive chemoradiotherapy is standard care in the management of unresectable EC. The lung is more susceptible to radiation damage than any other organ (2). Radiation pneumonitis (RP) is one of the most severe complications of radiotherapy (RT) or concurrent chemoradiotherapy for thoracic segment esophageal squamous cell carcinoma (TSESCC) (3), which seriously affects the implementation of tumor radiotherapy and the achievement of a curative effect. The most common clinical manifestations of RP are cough, shortness of breath, chest pain, and low-grade fever, which can be life-threatening in severe patients due to pulmonary failure (4).

A variety of risk factors have been reported to be associated with the development of RP, of which common include clinical features, dosimetric parameters, treatment-related factors as well as cytokines (2,5-8). Although the underlying mechanisms are not clear, it is currently recognized that RP is a complex process involving multiple cytokines, immune and inflammatory factors, especially inflammatory cytokines, which play an important role in leading to vascular endothelial and lung tissue injury (9). Clinical research has revealed that interleukin (IL)-1, IL-6, tumor necrosis factor (TNF)- α , transforming growth factor (TGF)- β , and platelet-derived growth factor (PDGF) are associated with the occurrence of RP (10). IL-6, the main proinflammatory interleukin of the acute lung response (11), induces the synthesis of acute-phase proteins, such as C-reactive protein (CRP), as well as other acute-phase reactants. Procalcitonin (PCT), as a precursor of calcitonin, is involved in systemic responses induced by circulating endotoxin and inflammatory cytokines. Studies have shown that PCT can distinguish infection from non-infection (12,13), and has a differential effect on RP and bacterial pneumonia (14). Although the above indicators are predictive of RP in lung cancer, they have not been applied for the prediction of RP in patients with TSESCC when treated by radiotherapy or concurrent chemoradiotherapy.

Since the symptoms in the early stage when RP occurs are often atypical, how to identify them early is still a significant clinical problem. In clinical practice, RP could be diagnosed by conventional computed tomography (CT) images which should be performed for differential diagnosis whenever suspicious symptoms of RP (cough,

fever, chest pain, or dyspnea) occur during or after radiotherapy. However, the CT imaging specificity changes were significantly delayed (3). Therefore, to identify the risk of RP could help to increase the irradiation dose of tumor while reduce normal tissue complication probability (NTCP). Consequently, there is an urgent clinical need for comprehensive indicators to be individualized and accurately predict RP. To this end, we developed a simple-to-use Nomogram combined with biological factors and clinical signs for individualized risk assessment and precise prediction of RP in patients with TSESCC treated by radiotherapy or concurrent chemoradiotherapy. We present the following article in accordance with the TRIPOD reporting checklist (available at <https://tcr.amegroups.com/article/view/10.21037/tcr-22-582/rc>).

Methods

Patients

A retrospective study was conducted on 174 patients with TSESCC who were pathologically diagnosed and treated with radiotherapy or concurrent chemoradiotherapy from October, 2013 to June, 2020 at the Zhongda Hospital affiliated with Southeast University. The inclusion criteria were as follows: (I) performance status (PS) (Eastern Cooperative Oncology Group, ECOG) score of ≤ 2 ; (II) no previous history of thoracic radiotherapy. The exclusion criteria were as follows: (I) previous pneumonectomy or lung metastasis; (II) patients with acute pulmonary infection, severe chronic bronchitis, emphysema, or pulmonale or other serious diseases (such as myocardial infarction within 6 months); (III) incomplete data due to loss of follow-up within 6 months after radiotherapy. The study was conducted in accordance with the Declaration of Helsinki (as revised in 2013). Informed consent was obtained from all patients. The study was approved by the ethics committee of Zhongda Hospital, Southeast University (No. 2019ZDSYLL002-Y03).

Radiotherapy

All patients received three-dimensional conformal radiotherapy (3DCRT) with one front field and two back oblique fields or fixed-field intensity modulated radiotherapy (IMRT). The radiotherapy target area used involved-field irradiation. The delineation of the target area was based on CT findings and other examination, such as positron emission

tomography-computed tomography (PET-CT) or upper gastrointestinal radiography. The gross tumor volume (GTV) was defined as the primary esophageal mass volume plus metastatic lymph node volumes in any imaging study. The clinical target volume (CTV) was defined to include a 5–8 mm margin surrounding the GTV and affected lymph node area. The planning target volume (PTV) margin was determined based on esophageal tumor movement on two-dimensional fluoroscopy. Treatment was delivered using 6MV-X-ray Primus-m linear accelerator. The prescribed doses were 40 to 60 Gy at 1.8 to 2.16 Gy per fraction once daily and 5 fractions per week. Organs at risk (OARs) referred to the Radiotherapy and Oncology Group (RTOG) guidelines.

Measurement of biomarkers in blood samples

Serum levels of IL-6, CRP and PCT were detected before radiotherapy (0 week) and at 2, 4, 6, and 12 weeks after radiotherapy. At first, blood specimens were centrifuged at 1,000 rpm for 15 min at 4 °C. Serum extracted was stored at –20 °C and tested in strict accordance with the kit instructions subsequently. Serum levels of IL-6 and PCT were detected by electrochemiluminescence using the COBAS8000 analyzer (Roche, Switzerland) and the relative kit. The serum levels of CRP were detected by nephelometry with the analyzer of SISTEMA BN II (Siemens, Germany) and the relative reagent kit.

Clinical signs and CT examination

The clinical data, imaging information, and laboratory test results were obtained from the medical records of the study institution. Specifically, clinical data included age, gender, ECOG PS, smoking status, tumor location, tumor node metastasis (TNM) stage [American Joint Commission on Cancer (AJCC) 8th edition], radiotherapy technique and dose, and adjuvant or concurrent chemotherapy. Prescribed dose, mean lung dose (MLD) and lung volume receiving more than 20 Gy (V20) were collected from dose volume histograms (DVHs). The nearest chest CT was collected before radiotherapy to assess the patient's lung condition. CT examination of the entire lung was performed using a multi-slice spiral technique with a slice thickness of 5 mm. CT imaging features was extracted by one of authors, while referring to the recommendations and CT reports of professional imaging physicians in our radiological institution. The imaging features (15) (reticular pattern,

ground-glass opacity, linear opacities, bronchiectasis, emphysema) were extracted to explore the influence of different imaging features on RP.

Evaluation of RP

Patients underwent chest CT for assessment during radiotherapy and 1, 3, and 6 months after radiotherapy. If suspicious symptoms of RP (such as cough, fever, chest tightness or dyspnea) occur during follow-up, laboratory tests and chest CT should be performed for differential diagnosis. The diagnosis of RP was mainly based on a history of radiotherapy in the past 6 months; symptoms such as cough, fever, or chest pain were present; patchy shadows, linear opacities, and honeycombs were observed around the irradiated lung; exclusion of pulmonary infection, pulmonary congestion and other diseases. RP was graded according to the National Cancer Institute Common Toxicity Criteria for Common Terminology Criteria for Adverse Events (CTCAE 5.0).

Statistical analysis and nomogram development

Data analysis was calculated using the Statistical Package for Social Sciences (SPSS for Windows, version 26.0) and R software (version 3.6.1). The χ^2 test was used to analyze categorical variables, and the Mann-Whitney U test was used for continuous variables that did not meet the normal distribution. P values on both sides <0.05 were considered statistically significant. In order to avoid ignoring important clinical features, factors with $P < 0.1$ in clinical features were analyzed by multivariate analysis. Correlation test was conducted before multivariate analysis to avoid multiple correlation between variables interfering with the accuracy of multivariate analysis. The variables with multiple correlations were screened by Lasso to obtain the variables with large contributions. Variables without multiple correlation can be analyzed directly by logistic regression analysis. Nomograms were constructed for factors that were statistically significant in the multivariate analysis (Figure S1). The area under the receiver operating characteristic (ROC) was used to evaluate the discrimination of the model. Calibration curves with 1,000 bootstrap resamples were used to compare predicted and actual probabilities, and clinical utility was assessed with decision curve analysis (DCA) (16). Besides, the web-based version of the dynamic nomogram was established to facilitate clinical utility.

Results

Patient characteristics and incidence of RP

Characteristics of the 174 eligible TSESCC patients are summarized in *Table 1*. Of these, the median age was 65 years (range, 21–89 years) and tumors were located in the middle and lower of thoracic esophagus mostly (77.6%). A total of 128 patients (73.6%) received concurrent chemoradiation or induction chemotherapy. Most patients (81.6%) were treated with IMRT. As for the dose parameters, the median of the prescribed dose was 46 Gy (range, 40–60 Gy) and median MLD, V20 of lung was 11.52 Gy, 21% respectively. According to CTCAE5.0, Grade 5 RP occurred in 1 case. The percentages of different grade RP were 14.3% (25 cases of grade 1), 12.6% (22 cases of grade 2), 2.87% (5 cases, grade 3), and 1.15% (2 cases grade 4), respectively. According to the time of occurrence of RP, among the 30 patients with RP (grade ≥ 2), there were 4 cases in 4 weeks of radiotherapy, 18 cases occurred between weeks 6 and 10, 4 cases in 12 weeks, 3 cases in 16 weeks and 1 case in 18 weeks. Univariate analysis showed that TNM stage and V20 were significantly associated with the risk of RP ($P < 0.05$).

Dynamic changes in cytokine levels during radiotherapy or concurrent chemoradiotherapy

The cytokine levels at pre-radiotherapy (0), and 2, 4, 6, and 12 weeks after radiotherapy initiation are presented in *Figure 1*. There were no differences in cytokine levels between the RP and non-RP group before radiotherapy. During radiotherapy or concurrent chemoradiotherapy, the levels of IL-6 and CRP in the RP group began to increase at 2 weeks, and reached the peak at 6 weeks, which was different from that in the non-RP group ($P < 0.05$). Unlike IL-6 and CRP, there was no significant difference in PCT levels between the two groups at different stages ($P > 0.05$).

Risk factors combined with biomarkers and clinical signs for RP

Spearman correlation analysis was performed on biomarkers and clinical signs associated with RP, indicating a strong correlation between cytokines. As shown in *Table S1* and *Figure 2*, the correlation coefficients between cytokines was 0.805 (IL-6_4W and IL-6_6W), 0.738 (IL-6_6W and CRP_6W), 0.741 (IL-6_6W and IL-6_12W), 0.713 (IL-6_6W and CRP_12W), 0.733 (CRP_12W

and CRP_6W) and 0.752 (CRP_12W and IL-6_12W) respectively. The correlation coefficient threshold between predictor variables of $|r| \geq 0.7$ was considered a suitable indicator when collinearity began to seriously distort model estimation and subsequent prediction (17,18). To lessen the multicollinearity, the least absolute shrinkage and selection operator (LASSO) algorithm was used to select the most valuable variable for RP discrimination by regulating the parameter λ . As shown in *Figure S2*, a 10-fold cross validation was performed. The following three features were screened from eight features according to the LASSO analysis (*Table S2*): IL-6 at 2 weeks, CRP at 6 weeks and CRP at 12 weeks. In clinical practice, most of the RP occurred between 6 and 10 weeks after radiotherapy which confirmed by CT with delayed specificity image changes (3). To be able to predict RP in time and reduce the effect of multicollinearity on the model, cytokine levels in CRP at 12 weeks were not used for prediction. Multivariate analysis was performed for clinical factors with $P < 0.1$ in univariate analysis and cytokines selected by lasso. Multivariate logistic regression analysis identified the IL-6 at 2 weeks, CRP at 6 weeks and RT techniques as independent predictors (*Table 2*).

A simple-to-use nomogram developed for prediction the risk of RP

Based on the multivariate analysis, a simple-to-use nomogram model was built to predict the risk of RP, which included IL-6 at 2 weeks, CRP at 6 weeks and RT techniques (*Figure 3A*). To facilitate clinical use, we developed a dynamic nomogram using the “Dynnom” package of R software, this dynamic model is available at this web address (<https://qtnomogram.shinyapps.io/dynnomapp/>). The left interface of the dynamic nomogram can set parameters, and the probability and confidence interval of RP occurrence are displayed in the right interface (*Figure 3B*). The area under the curve (AUC) of the predictive model was 0.898 [95% confidence interval (CI): 0.849–0.9475], which was superior to each predictor alone (RT techniques: 0.570, 95% CI: 0.452–0.688; IL-6_2W: 0.808, 95% CI: 0.725–0.891; and CRP_6W: 0.819, 95% CI: 0.740–0.897) (*Figure 4A*). The sensitivity of this model was 0.967 and the specificity was 0.736. The cutoff values of IL-6_2W and CRP_6W were 19.17 pg/mL and 30.25 mg/L, respectively. Additionally, the calibration curve (1,000 bootstrap resamples) showed favorable agreement between the prediction by nomogram and the actual observation

Table 1 Patients characteristics (n=174)

Clinical feature	Sum, n (%)	RP, n (%)	Non-RP, n (%)	χ^2	P
Age (years)				0.461	0.497
<65	91 (52.2)	14 (46.7)	77 (53.5)		
≥65	83 (47.8)	16 (53.3)	67 (46.5)		
Sex				2.724	0.098
Male	130 (74.7)	26 (86.7)	104 (72.2)		
Female	44 (25.3)	4 (13.3)	40 (27.8)		
PS				0.1	0.751
0–1	151 (86.8)	25 (83.3)	126 (87.5)		
2	23 (13.2)	5 (16.7)	18 (12.5)		
Smoking				1.924	0.165
Yes	62 (35.6)	14 (46.7)	48 (33.3)		
No	112 (64.4)	16 (53.3)	96 (66.7)		
TNM stage				8.94	0.003*
I–II	65 (37.4)	4 (13.3)	61 (42.4)		
III–IV	109 (62.6)	26 (86.7)	83 (57.6)		
Position				2.55	0.279
Upper	39 (22.4)	6 (20.0)	33 (23.0)		
Middle	86 (49.4)	12 (40.0)	74 (51.3)		
Lower	49 (28.2)	12 (40.0)	37 (25.7)		
COPD				3.154	0.076
Yes	37 (21.3)	10 (33.3)	27 (18.8)		
No	137 (78.7)	20 (66.7)	117 (81.2)		
Reticular pattern				0.743	0.607
Yes	16 (9.2)	4 (13.3)	12 (8.3)		
No	158 (90.8)	26 (86.7)	132 (91.7)		
Ground-glass opacity				0.251	0.616
Yes	57 (32.8)	11 (36.7)	46 (31.9)		
No	117(67.2)	19 (63.3)	98 (68.1)		
Linear opacities				0.407	0.523
Yes	113 (64.9)	21 (70.0)	92 (63.9)		
No	61 (35.1)	9 (30.0)	52 (36.1)		
Bronchiectasis				0.003	1.000
Yes	12 (6.9)	2 (6.7)	10 (6.9)		
No	162 (93.1)	28 (93.3)	134 (93.1)		

Table 1 (continued)

Table 1 (continued)

Clinical feature	Sum, n (%)	RP, n (%)	Non-RP, n (%)	χ^2	P
Emphysema				0.6	0.438
Yes	59 (33.9)	12 (40.0)	47 (32.6)		
No	115 (66.1)	18 (60.0)	97 (67.4)		
RT techniques				3.255	0.071
3DCRT	32 (18.4)	9 (30.0)	23 (16.0)		
IMRT	142 (81.6)	21 (70.0)	121 (84.0)		
MLD (Gy)				0.659	0.417
<13	121 (69.5)	19 (63.3)	102 (70.8)		
≥13	53 (30.5)	11 (36.7)	42 (29.2)		
Prescribed dose (Gy)				0.71	0.399
<54	166 (95.4)	30 (100.0)	136 (94.4)		
≥54	8 (4.6)	0 (0.0)	8 (5.6)		
V20 (%)				4.139	0.042*
<25	120 (69.0)	16 (53.3)	104 (72.2)		
≥25	54 (31.0)	14 (46.7)	40 (27.8)		
Chemotherapy				1.779	0.182
Yes	128 (73.6)	25 (83.3)	103 (71.5)		
No	46 (26.4)	5 (16.7)	41 (28.5)		

*P<0.05. RP, radiation pneumonitis; PS, performance status; COPD, chronic obstructive pulmonary disease; RT, radiotherapy; 3DCRT, three-dimensional conformal radiotherapy; IMRT, intensity modulated radiotherapy; MLD, mean lung dose; V20, lung volume receiving more than 20 Gy.

(Figure 4B). Furthermore, DCA showed a good positive net benefit at most threshold probabilities, indicating excellent clinical utility (Figure 4C). Figure 5 shows a typical case that dynamically shows cytokines and chest CT changes during radiotherapy. In this case, a 66-year-old patient with TSESCC received three-dimensional conformal radiotherapy (3DCRT) with a prescription dose of 50 Gy/25 F between November 12, 2019, and December 16, 2019. One month after the end of radiotherapy (January 11, 2020), he developed the cough with chest tightness. Chest CT in our hospital showed scattered interstitial changes in both lungs, especially in the irradiation field (Figure 5D-5F). PCT was 0.104 ng/mL, IL-6 was 54.5 pg/mL, and CRP was 125 mg/L. RP was considered in combination with patient's medical history and auxiliary examination. After glucocorticoid treatment, the patient's chest tightness and cough symptoms were significantly

improved. Repeat chest CT (January 19, 2020) showed that the interstitial change was significantly absorbed than before (Figure 5G-5I). PCT was 0.092 ng/mL, IL-6 was 23.21 pg/mL, and CRP was 24.3 mg/L. A review of the radiotherapy process showed that during the radiotherapy period (2 and 6 weeks), IL-6 and CRP were higher than normal levels. IL-6 was 22.7 and 27.6 pg/mL, respectively, and CRP was 11.1 and 69.2 mg/L, while PCT was within the normal range. At this time (December 10, 2019), CT imaging showed no inflammatory exudation (Figure 5A-5C), and the patient had no fever, cough, chest pain, dyspnea or other infectious symptoms. The nomogram in this paper predicts 89.9% probability of RP in this patient. Therefore, patients who receive 3DCRT radiotherapy, with persistently elevated IL-6 and CRP above the normal range in plasma during treatment (2 weeks, 6 weeks), should be alert to the occurrence of RP.

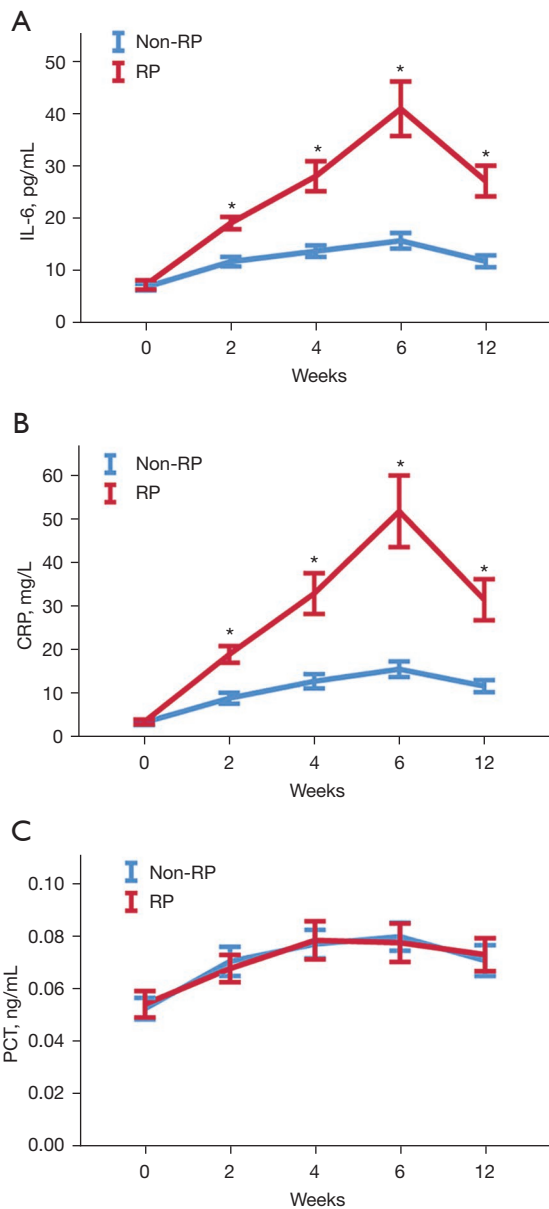


Figure 1 Changes in the levels of IL-6, CRP and PCT in plasma of patients during treatment and follow-up. (A) The serum levels of IL-6 were statistically different after 2 weeks between RP group and non-RP group ($P < 0.05$). (B) The CRP levels in the plasma of the RP group showed a significant difference from those of the non-RP group after 2 weeks ($P < 0.05$). (C) The levels of PCT showed no significant difference comparing the RP group to non-RP groups ($P > 0.05$) during radiotherapy or concurrent chemoradiotherapy. * $P < 0.05$. IL-6, interleukin-6; CRP, C-reactive protein; PCT, procalcitonin; RP, radiation pneumonitis.

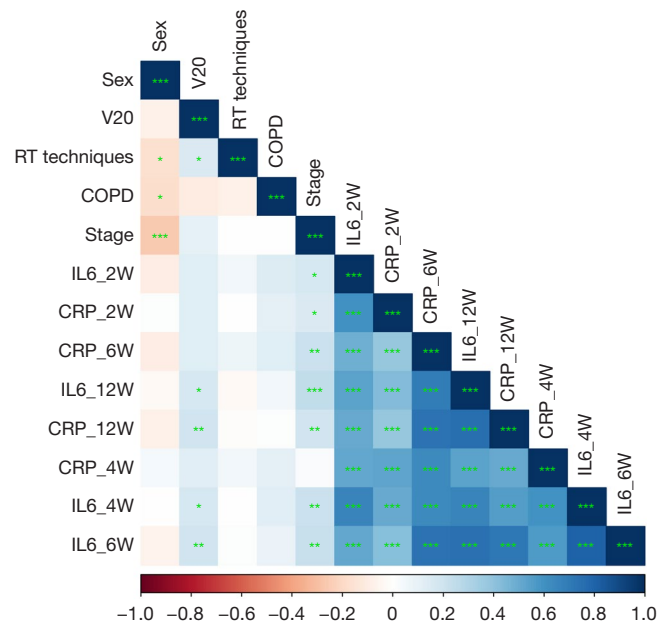


Figure 2 The correlation of biomarkers cytokines, dosimetric performance, and clinical signs. Blue indicates positive correlation, red indicates negative correlation, and the shade of color represents the strength of the correlation. For the P value of correlation analysis, “*”, “**” and “***” are used to represent “ $P < 0.05$ ”, “ $P < 0.01$ ”, “ $P < 0.001$ ”, respectively. COPD, chronic obstructive pulmonary disease; V20, percentage of total lungs volume receiving 20 Gy; IL-6, interleukin-6; CRP, C-reactive protein; W, week; RT, radiotherapy.

Table 2 Multivariate analysis of risk factor for RP

Intercept and variable	β	Odds ratio (95% CI)	P
Intercept	-7.210	-	<0.000
IL6_2W	0.178	1.194 (1.072–1.330)	0.001*
CRP_6W	0.034	1.035 (1.016–1.053)	0.000*
COPD	0.409	1.505 (0.436–5.200)	0.518
Stage	1.028	2.795 (0.714–10.938)	0.140
Sex	-0.483	0.492 (0.156–2.444)	0.492
V20	0.797	2.219 (0.742–6.637)	0.154
RT techniques	1.911	6.757 (1.848–24.71)	0.004*

* $P < 0.05$. RP, radiation pneumonitis; IL-6, interleukin-6; CRP, C-reactive protein; W, week; COPD, chronic obstructive pulmonary disease; V20, lung volume receiving more than 20 Gy; RT, radiotherapy.

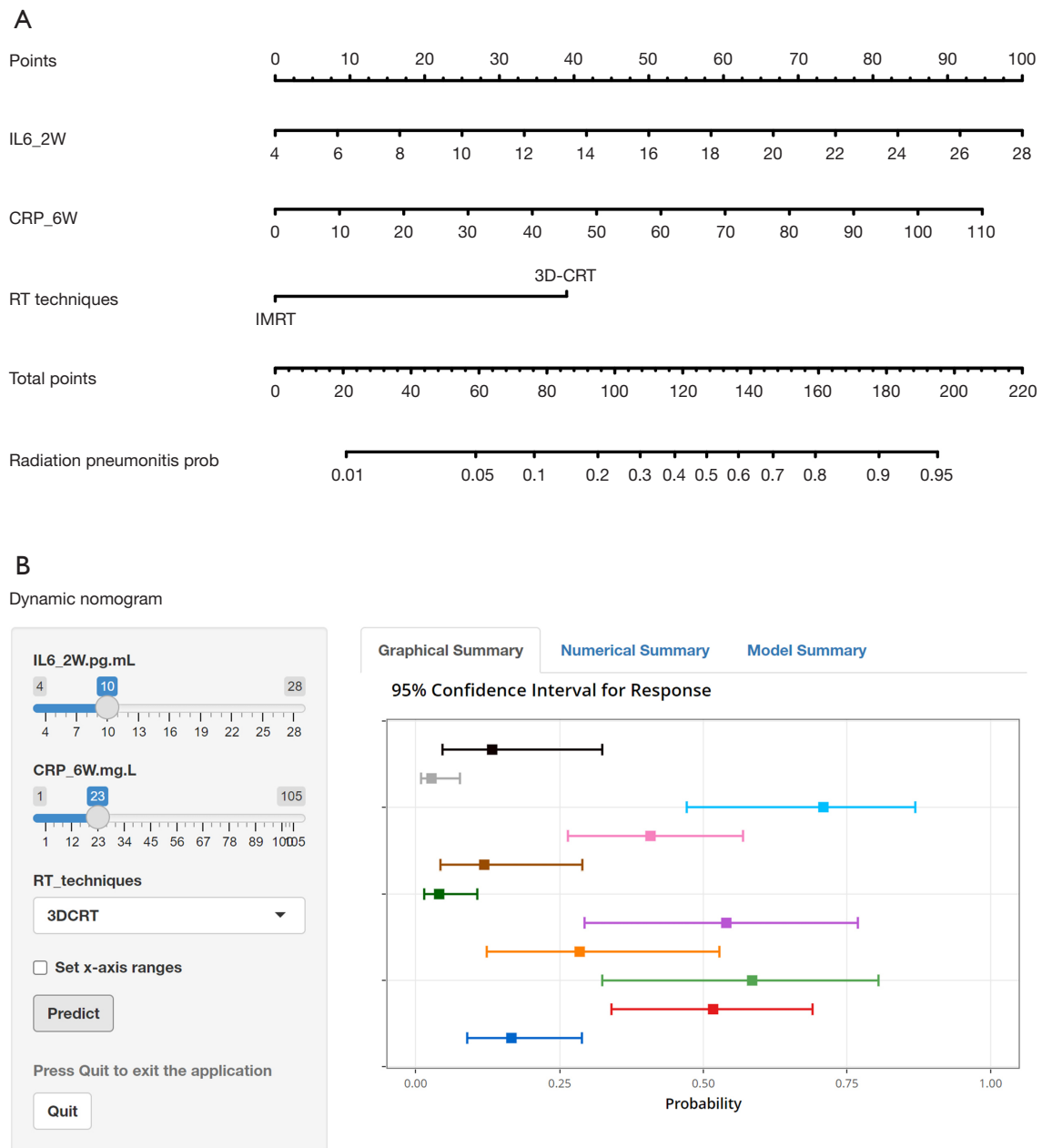


Figure 3 A simple-to-use nomogram for prediction the risk of RP. (A) The nomogram was developed incorporating the IL-6 at 2 weeks, CRP at 6 weeks, and RT techniques. (B) Operation interface of nomogram on the web page. The corresponding probability of RP can be obtained by inputting IL-6_2W, CRP_6W and RT techniques (IMRT or 3DCRT) on the left side of the patient. RP, radiation pneumonitis; IL-6, interleukin-6; CRP, C-reactive protein; W, week; RT, radiotherapy; IMRT, intensity modulated radiotherapy; 3DCRT, three-dimensional conformal radiotherapy.

Discussion

RP represents the acute expression of radio-induced lung damage and is a limiting toxicity affecting its therapeutic

outcome (4). As a common side effect of radiotherapy for EC, its incidence is 5.7–35.0% (2,19,20), and the incidence of RP (grade ≥ 2) in this study was 17.2%, which is consistent

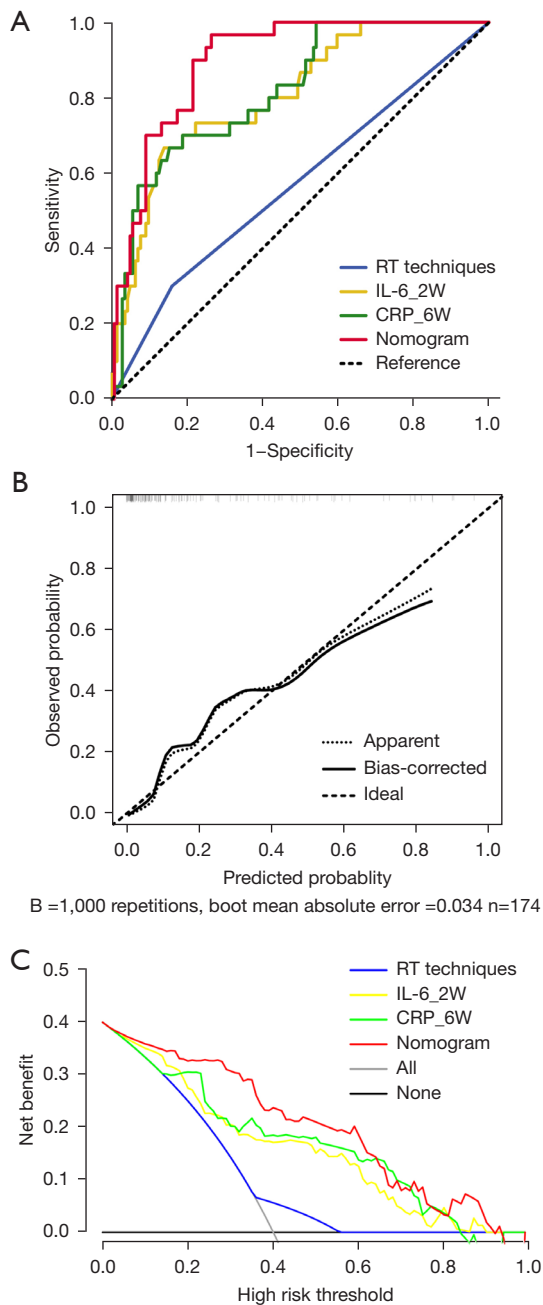


Figure 4 Predictive performance of the nomogram. (A) ROC curves of IL-6_2W, CRP_6W, RT techniques. (B) Calibration curve of the nomogram predicting the risk of radiation pneumonitis. The x-axis and y-axis indicate the predicted and actual probabilities of radiation pneumonitis, respectively. (C) Decision curves of IL-6_2W, CRP_6W, RT techniques and the prediction model predicting RP. The x-axis represents the threshold probability, and the y-axis represents the net benefit rate after the benefit minus the hazard. ROC, receiver operating characteristic curve.

with previous studies. We also found that RP occurred mostly 6–10 weeks after radiotherapy, and 18 patients in this study developed grade ≥ 2 RP within 6–10 weeks (60%), similar to the results of prospective clinical study, in which the incidence of RP reached 44% within 6–8 weeks of treatment (21).

The exact molecular mechanism of RP is still unclear because of its complex pathological mechanisms. According to the current understanding (8,22), damaged epithelial cells and endothelial cells produce a series of damage-associated molecular patterns (DAMPs), release a large number of cytokines, activate immune cells, and these factors interact to lead to the occurrence of RP. RP could have an evolutionary trend with signs occurring at hours to days of immune cell infiltration damage to type I pneumocyte releasing cytokines; followed by weeks to months of inflammatory cells recruitment by cytokines leading to pneumonitis (2). Several studies have evaluated cytokine levels associated with lung damage secondary to radiation exposure and have reported that cytokines play an indispensable role in the development of RP (5-8,10,23,24). However, it is difficult to select the most appropriate cytokine among numerous cytokines able to predict RP. The main proinflammatory interleukins of acute lung response are IL-1 and IL-6 (11). A prospective study investigated changes in IL-6, IL-10, and TNF- α at baseline, every 2 weeks during radiotherapy, and at the end of radiotherapy. In their study, the changes of IL-6 and IL-10 were significantly different between RP and non-RP groups after 2 weeks of radiotherapy. They suggested that early changes in IL-6 and IL-10 levels, especially opposing variations in these cytokines, may be relevant as predictors of RP (21). Several studies have shown that IL-6 has a discriminatory role between RP and non-RP (5,21,23). Jeong *et al.* (5) reported that IL-6 levels were significantly increased in the plasma of patients 3 weeks after radiotherapy and proposed the importance of early changes in cytokine levels for predicting the development and severity of RP. Accordingly, this study not only found early changes in IL-6, but also found the same changes in CRP. This phenomenon occurs because IL-6, as a key cytokine in the inflammatory response, can induce the synthesis of acute phase proteins such as CRP (25). Similarly, in a recent study of patients with RP treated with glucocorticoids (9), it was found that the therapeutic effects improved as CRP levels decreased significantly. In addition, at the onset of RP, the number of CD4⁺ T cells was significantly reduced and CRP levels were correspondingly increased as the degree of RP injury

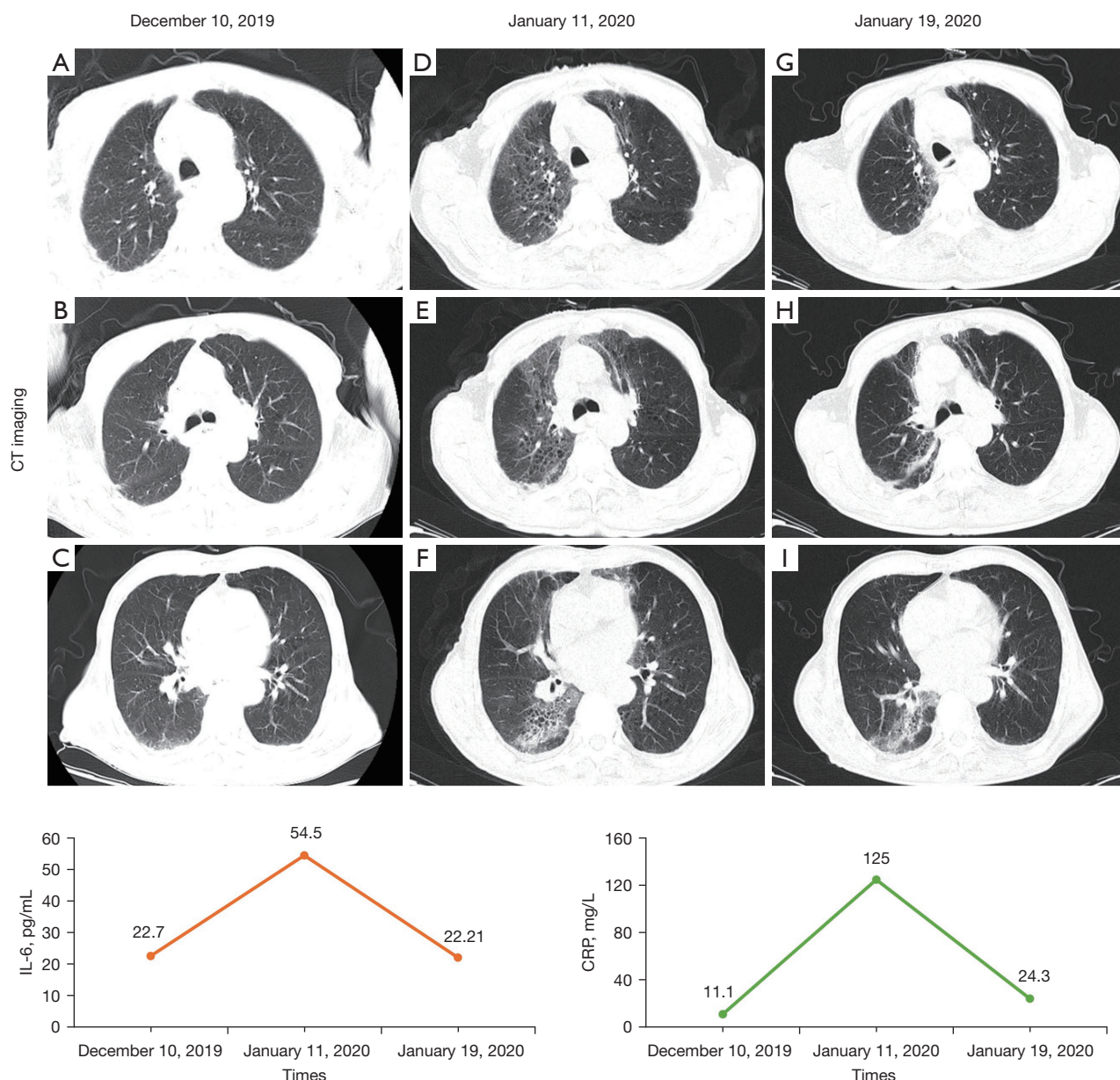


Figure 5 A typical case of the chest CT imaging and interleukin-6 dynamic changes in patients with TSESCC after radiotherapy. (A-C) Lung imaging when cytokines were altered; (D-F) scattered interstitial changes in both lungs at the onset of radiation pneumonitis; (G-I) interstitial changes after glucocorticoid treatment are more absorbed than before. Dynamic changes of IL-6 and CRP in plasma. CT, computed tomography; IL-6, interleukin-6; CRP, C-reactive protein; PCT, procalcitonin.

increased. As expected, PCT levels were consistent between patients with and without RP during radiotherapy and during follow-up, because RP is an aseptic inflammation essentially. However, no prediction model for IL-6 has been established. Additionally, the inflammatory state is not static, dynamic analysis may be more informative. Therefore, the

present study employed dynamic monitoring of cytokine during radiotherapy or concurrent chemoradiotherapy. IL-6 and CRP were found to be effective predictors of RP.

With the development of imaging technology and the rise of radiomics, increasing studies have focused on combining radiomics with clinical features to predict the

occurrence of RP (20,26,27). However, the repeatability of features is doubtful as the equipment model varies from hospital to hospital. Thus, we adopted the traditional imaging extraction method to extract the imaging features. Imaging signs were defined according to the 2008 Fleischner Society Guide to the Glossary of Chest Imaging (15), and included reticular pattern, ground-glass opacity, linear opacities, bronchiectasis, and emphysema. In our study, we extracted the features of the chest CT of the patients before radiotherapy. Lee *et al.* observed interstitial change in the pre-radiation therapy chest CT scan was the only clinical factor associated with RP (28). Pulmonary fibrosis is positively correlated with RP in patients with EC, suggesting that pulmonary fibrosis is an independent risk factor for RP (grade =3) (29). However, there was no statistically significant difference in interstitial pneumonitis-related characteristics in our study. We consider the reason for this phenomenon to be related to the separate analysis of each feature of pulmonary fibrosis.

Lee *et al.* recommend that MLD and V20 can predict RP effectively with cutoffs of 13.6 Gy and 25%, respectively (30). Tonison *et al.* recommend limiting lung V20 to less than 23% in EC patients undergoing chemoradiation, the risk of developing grade 2 or higher RP would be less than 10% (31). However, a study (32) on RP suggested that V20 was associated with the occurrence of RP, but it was not an independent risk factor for the development of RP, similar to the results of this study. Dosimetric risk factors are mostly based on lung cancer development. For example, a large meta-analysis on the occurrence of RP after chemoradiotherapy for lung cancer (33), it was proposed that V20 was associated with the occurrence of symptomatic RP independently. The study also concluded that patients older than 65 years had the highest risk of RP when receiving carboplatin/paclitaxel. However, disease and treatment-specific factors, as well as anatomical, differences between lung and esophageal tumors limit the transferability of risk factors from pulmonary to esophageal tumors. Thus, the risk factors of RP in EC still need to be further confirmed by prospective studies. In our study, radiotherapy technique with 3DCRT was found to be an independent risk factor for developing RP. In a comparative article on the efficacy of IMRT and 3DCRT for EC, it was demonstrated that IMRT could improve the survival rate and reduce the risk of RP compared with 3DCRT (34). Similarly, in the study by Lan *et al.*, it was considered that the use of 3DCRT radiotherapy technique

was an independent risk factor for the development of RP (19). This may be associated with the ability of IMRT compared to 3DCRT to provide precise target coverage, reduce dose inhomogeneity and toxicity to normal organs (35). However, 3DCRT was not a risk factor in a predictive model for RP in EC (29). Inflammatory factors, such as systemic immune inflammation index (SII), platelet-lymphocyte ratio (PLR), lymphocyte-monocyte ratio (LMR) and neutrophils-lymphocyte ratio (NLR), were also analyzed in their article. Among them, the rate of change of SII at four weeks was an independent risk factor for RP. The model was also validated internally and externally, with a predictive model C-index of 0.852. In our study, CRP and IL-6 were used to predict RP, and the predictive model C-index was 0.898, while providing a dynamic web prediction model to facilitate clinical use. We will perform external validation of the model in subsequent studies while comparing the above inflammatory indicators to obtain the best predictive model. In the present study, TNM stage was a risk factor but not an independent risk factor for RP. Thus, it not included in our model.

Hereafter, in our study, several significant variables including IL-6 at 2 weeks, CRP at 6 weeks and RT techniques were integrated into a nomogram to provide an accurate individualized risk assessment of RP for each patient. However, several limitations should be discussed. First, as this was a retrospective study with a small sample size, selection bias might be present. Second, 75% of patients in this study had received chemotherapy with prescribed RT dose is ranged from 40 to 60 Gy. This may lead to some heterogeneity in the data. Third, the prescription dose of this study is relatively low, which may limit the generalization of the model to a certain extent. Therefore, we will use multi-center, large-sample data to continuously improve the model in the follow-up research.

Conclusions

This study presents a nomogram that incorporates RT techniques, IL-6 and CRP to effectively predict the risk of RP in patients with TSESSC treated by radiotherapy or concurrent chemoradiotherapy. This simple-to-use nomogram may be considered for practice in clinical care.

Acknowledgments

Funding: None.

Footnote

Reporting Checklist: The authors have completed the TRIPOD reporting checklist. Available at <https://tcr.amegroups.com/article/view/10.21037/tcr-22-582/rc>

Data Sharing Statement: Available at <https://tcr.amegroups.com/article/view/10.21037/tcr-22-582/dss>

Peer Review File: Available at <https://tcr.amegroups.com/article/view/10.21037/tcr-22-582/prf>

Conflicts of Interest: All authors have completed the ICMJE uniform disclosure form (available at <https://tcr.amegroups.com/article/view/10.21037/tcr-22-582/coif>). The authors have no conflicts of interest to declare.

Ethical Statement: The authors are accountable for all aspects of the work in ensuring that questions related to the accuracy or integrity of any part of the work are appropriately investigated and resolved. The study was conducted in accordance with the Declaration of Helsinki (as revised in 2013). Informed consent was obtained from all patients. The study was approved by the ethics committee of Zhongda Hospital, Southeast University (No. 2019ZDSYLL002-Y03).

Open Access Statement: This is an Open Access article distributed in accordance with the Creative Commons Attribution-NonCommercial-NoDerivs 4.0 International License (CC BY-NC-ND 4.0), which permits the non-commercial replication and distribution of the article with the strict proviso that no changes or edits are made and the original work is properly cited (including links to both the formal publication through the relevant DOI and the license). See: <https://creativecommons.org/licenses/by-nc-nd/4.0/>.

References

- Sung H, Ferlay J, Siegel RL, et al. Global Cancer Statistics 2020: GLOBOCAN Estimates of Incidence and Mortality Worldwide for 36 Cancers in 185 Countries. *CA Cancer J Clin* 2021;71:209-49.
- Ullah T, Patel H, Pena GM, et al. A contemporary review of radiation pneumonitis. *Curr Opin Pulm Med* 2020;26:321-5.
- Simone CB 2nd. Thoracic Radiation Normal Tissue Injury. *Semin Radiat Oncol* 2017;27:370-7.
- Jain V, Berman AT. Radiation Pneumonitis: Old Problem, New Tricks. *Cancers (Basel)* 2018;10:222.
- Jeong BK, Kim JH, Jung MH, et al. Cytokine Profiles of Non-Small Cell Lung Cancer Patients Treated with Concurrent Chemoradiotherapy with Regards to Radiation Pneumonitis Severity. *J Clin Med* 2021;10:699.
- Nishimoto N. Interleukin-6 as a therapeutic target in candidate inflammatory diseases. *Clin Pharmacol Ther* 2010;87:483-7.
- Hanania AN, Mainwaring W, Ghebre YT, et al. Radiation-Induced Lung Injury: Assessment and Management. *Chest* 2019;156:150-62.
- Käsmann L, Dietrich A, Staab-Weijnitz CA, et al. Radiation-induced lung toxicity - cellular and molecular mechanisms of pathogenesis, management, and literature review. *Radiat Oncol* 2020;15:214.
- Bai L, Zhou BS, Zhao YX. Dynamic changes in T-cell subsets and C-reactive protein after radiation therapy in lung cancer patients and correlation with symptomatic radiation pneumonitis treated with steroid therapy. *Cancer Manag Res* 2019;11:7925-31.
- Guo L, Ding G, Xu W, et al. Prognostic biological factors of radiation pneumonitis after stereotactic body radiation therapy combined with pulmonary perfusion imaging. *Exp Ther Med* 2019;17:244-50.
- Yu HH, Chengchuan Ko E, Chang CL, et al. Fucoidan Inhibits Radiation-Induced Pneumonitis and Lung Fibrosis by Reducing Inflammatory Cytokine Expression in Lung Tissues. *Mar Drugs* 2018;16:392.
- Walsh TL, DiSilvio BE, Hammer C, et al. Impact of Procalcitonin Guidance with an Educational Program on Management of Adults Hospitalized with Pneumonia. *Am J Med* 2018;131:201.e1-8.
- Contou D, d'Ythurbide G, Messika J, et al. Description and predictive factors of infection in patients with chronic kidney disease admitted to the critical care unit. *J Infect* 2014;68:105-15.
- Wang Z, Huo B, Wu Q, et al. The role of procalcitonin in differential diagnosis between acute radiation pneumonitis and bacterial pneumonia in lung cancer patients receiving thoracic radiotherapy. *Sci Rep* 2020;10:2941.
- Hansell DM, Bankier AA, MacMahon H, et al. Fleischner Society: glossary of terms for thoracic imaging. *Radiology* 2008;246:697-722.
- Fitzgerald M, Saville BR, Lewis RJ. Decision curve analysis. *JAMA* 2015;313:409-10.
- Vatcheva KP, Lee M, McCormick JB, et al.

- Multicollinearity in Regression Analyses Conducted in Epidemiologic Studies. *Epidemiology* (Sunnyvale) 2016.
18. Dormann CF, Elith J, Bacher S, et al. Collinearity: a review of methods to deal with it and a simulation study evaluating their performance. *Ecography* 2013;36:27-46.
 19. Lan K, Xu C, Liu S, et al. Modeling the risk of radiation pneumonitis in esophageal squamous cell carcinoma treated with definitive chemoradiotherapy. *Esophagus* 2021;18:861-71.
 20. Wang L, Gao Z, Li C, et al. Computed Tomography-Based Delta-Radiomics Analysis for Discriminating Radiation Pneumonitis in Patients With Esophageal Cancer After Radiation Therapy. *Int J Radiat Oncol Biol Phys* 2021;111:443-55.
 21. Arpin D, Perol D, Blay JY, et al. Early variations of circulating interleukin-6 and interleukin-10 levels during thoracic radiotherapy are predictive for radiation pneumonitis. *J Clin Oncol* 2005;23:8748-56.
 22. Hansel C, Jendrossek V, Klein D. Cellular Senescence in the Lung: The Central Role of Senescent Epithelial Cells. *Int J Mol Sci* 2020;21:3279.
 23. Fu ZZ, Peng Y, Cao LY, et al. Correlations Between Serum IL-6 Levels and Radiation Pneumonitis in Lung Cancer Patients: A Meta-Analysis. *J Clin Lab Anal* 2016;30:145-54.
 24. Shen ZT, Shen JS, Ji XQ, et al. TGF- β 1 rs1982073 polymorphism contributes to radiation pneumonitis in lung cancer patients: a meta-analysis. *J Cell Mol Med* 2016;20:2405-9.
 25. Lu ZY, Brailly H, Wijdenes J, et al. Measurement of whole body interleukin-6 (IL-6) production: prediction of the efficacy of anti-IL-6 treatments. *Blood* 1995;86:3123-31.
 26. Du F, Tang N, Cui Y, et al. A Novel Nomogram Model Based on Cone-Beam CT Radiomics Analysis Technology for Predicting Radiation Pneumonitis in Esophageal Cancer Patients Undergoing Radiotherapy. *Front Oncol* 2020;10:596013.
 27. Krafft SP, Rao A, Stingo F, et al. The utility of quantitative CT radiomics features for improved prediction of radiation pneumonitis. *Med Phys* 2018;45:5317-24.
 28. Lee YH, Kim YS, Lee SN, et al. Interstitial Lung Change in Pre-radiation Therapy Computed Tomography Is a Risk Factor for Severe Radiation Pneumonitis. *Cancer Res Treat* 2015;47:676-86.
 29. Wang L, Liang S, Li C, et al. A Novel Nomogram and Risk Classification System Predicting Radiation Pneumonitis in Patients With Esophageal Cancer Receiving Radiation Therapy. *Int J Radiat Oncol Biol Phys* 2019;105:1074-85.
 30. Lee HJ Jr, Zeng J, Vesselle HJ, et al. Correlation of Functional Lung Heterogeneity and Dosimetry to Radiation Pneumonitis using Perfusion SPECT/CT and FDG PET/CT Imaging. *Int J Radiat Oncol Biol Phys* 2018;102:1255-64.
 31. Tonison JJ, Fischer SG, Viehrig M, et al. Radiation Pneumonitis after Intensity-Modulated Radiotherapy for Esophageal Cancer: Institutional Data and a Systematic Review. *Sci Rep* 2019;9:2255.
 32. Tang W, Li X, Yu H, et al. A novel nomogram containing acute radiation esophagitis predicting radiation pneumonitis in thoracic cancer receiving radiotherapy. *BMC Cancer* 2021;21:585.
 33. Palma DA, Senan S, Tsujino K, et al. Predicting radiation pneumonitis after chemoradiation therapy for lung cancer: an international individual patient data meta-analysis. *Int J Radiat Oncol Biol Phys* 2013;85:444-50.
 34. Lan K, Zhu J, Zhang J, et al. Propensity score-based comparison of survival and radiation pneumonitis after definitive chemoradiation for esophageal cancer: Intensity-modulated radiotherapy versus three-dimensional conformal radiotherapy. *Radiother Oncol* 2020;149:228-35.
 35. Chen NB, Qiu B, Zhang J, et al. Intensity-Modulated Radiotherapy versus Three-Dimensional Conformal Radiotherapy in Definitive Chemoradiotherapy for Cervical Esophageal Squamous Cell Carcinoma: Comparison of Survival Outcomes and Toxicities. *Cancer Res Treat* 2020;52:31-40.

Cite this article as: Qiu T, Deng Y, Guo H, Zhang H. A simple-to-use nomogram for predicting the risk of radiation pneumonitis in patients with thoracic segment esophageal squamous cell carcinoma. *Transl Cancer Res* 2022;11(10):3754-3766. doi: 10.21037/tcr-22-582

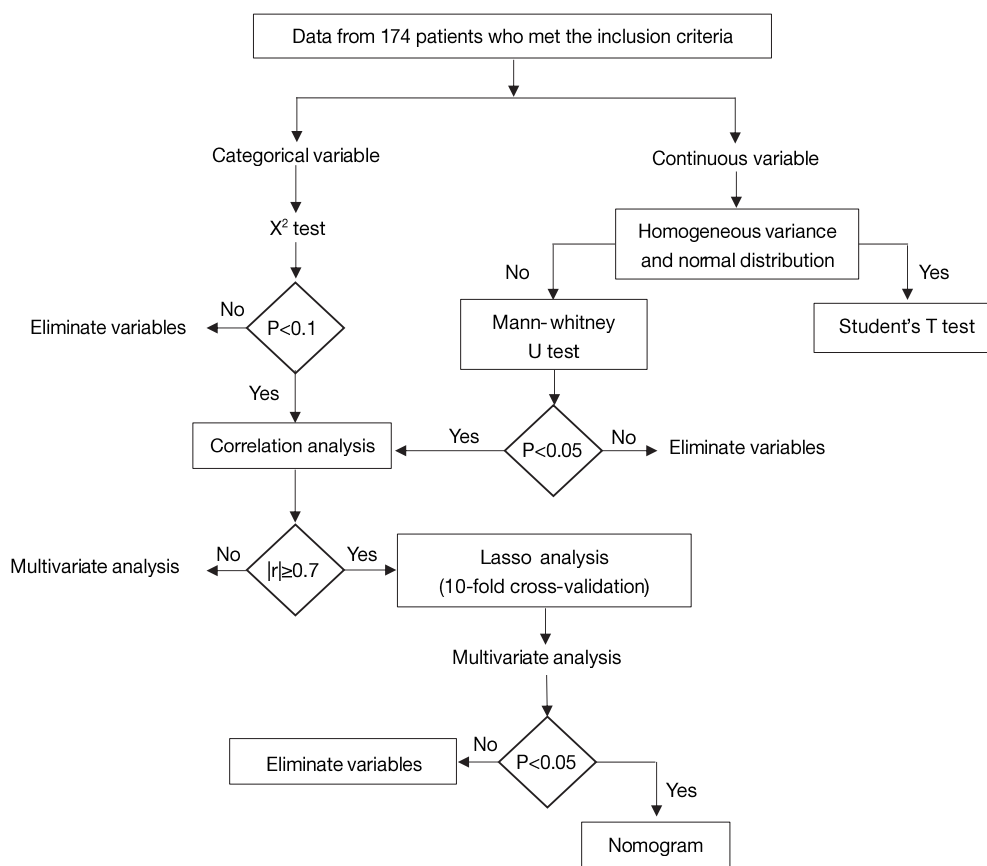


Figure S1 Flow chart of data analysis.

Table S1 The correlation coefficient of cytokines, dosimetric performance, and clinical signs

	Sex	COPD	V20	Stage	RT techniques	IL6_2W	CRP_2W	IL6_4W	CRP_4W	IL6_6W	CRP_6W	IL6_12W	CRP_12W
Sex	1.000	0.173	-0.075	-0.261	-0.167	-0.090	0.011	0.008	0.048	-0.064	-0.094	-0.038	-0.075
COPD	-0.173	1.000	0.157	-0.005	-0.079	0.145	0.116	0.120	0.111	0.085	0.137	0.053	0.016
V20	-0.075	-0.105	1.000	0.107	0.158	0.137	0.130	0.173	0.128	0.197	0.139	0.177	0.198
Stage	0.261	-0.005	0.107	1.000	0.001	0.174	0.157	0.211	0.024	0.229	0.210	0.248	0.198
RT techniques	0.167	-0.079	0.158	0.001	1.000	0.058	-0.004	-0.000	0.053	0.016	0.076	-0.033	-0.013
IL6_2W	0.090	0.145	0.137	0.174	0.058	1.000	0.605	0.650	0.515	0.516	0.482	0.536	0.506
CRP_2W	0.101	0.116	0.130	0.157	-0.004	0.605	1.000	0.506	0.527	0.429	0.383	0.430	0.383
IL6_4W	0.008	0.120	0.173	0.211	0.000	0.650	0.506	1.000	0.590	0.805	0.633	0.656	0.554
CRP_4W	0.048	0.111	0.128	0.241	0.053	0.515	0.527	0.590	1.000	0.562	0.634	0.534	0.508
IL6_6W	0.646	0.085	0.197	0.229	0.016	0.516	0.429	0.805	0.562	1.000	0.738	0.741	0.713
CRP_6W	0.094	0.137	0.139	0.210	0.076	0.482	0.383	0.633	0.634	0.738	1.000	0.693	0.733
IL6_12W	0.038	0.053	-0.177	0.248	0.033	0.536	0.430	0.656	0.534	0.741	0.693	1.000	0.752
CRP_12W	0.075	0.016	-0.198	0.198	-0.013	0.506	0.383	0.554	0.508	0.713	0.733	0.752	1.000

COPD, chronic obstructive pulmonary disease; MLD, mean dose of total lungs; V20, lungs volume receiving more than 20 Gy; IL-6, interleukin-6; CRP, C-reactive protein; W, week; RT, radiotherapy.

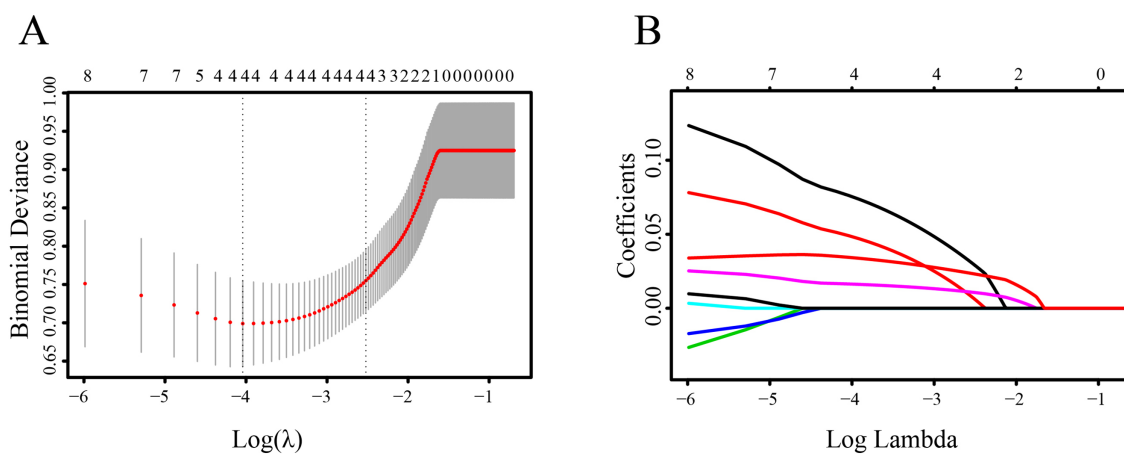


Figure S2 Feature selection using LASSO analysis. (A) Selection of the tuning parameter (λ) in the LASSO analysis used 10-fold cross-validation. The two dashed lines were drawn at the optimal values by using the minimum criteria and the 1 standard error of the minimum criteria (the 1-SE criteria). The model based on the 1-SE criteria is optimal. (B) Regression coefficients for 8 variables. As λ increases, the coefficient value of each variable gradually approaches zero.

Table S2 LASSO analysis

Characteristics	Coefficient
Intercept	-2.470472411
IL6_2W	0.013929215
CRP_2W	0
IL6_4W	0
CRP_4W	0
IL6_6W	0
CRP_6W	0.008858466
IL6_12W	0
CRP_12W	0.020841995

The optimal λ (1-SE criteria) was used to obtain the exact value of the final regression coefficient, and the optimal λ was obtained after ten-fold cross-validation.